High-Efficiency Si/Polymer Hybrid Solar Cells Based on Synergistic Surface Texturing of Si Nanowires on Pyramids

Lining He, Donny Lai, Hao Wang, Changyun Jiang, and Rusli**

Among the major long-term concerns facing the world, there are few as deserving of undivided attention as that of the ever-increasing global demand for renewable energy such as solar radiation. Unfortunately, the high production cost of the conventional Si solar cells poses a barrier for solar energy to compete with fossil fuels. In the past few years, there has been significant interest in the study of silicon nanowire (SiNW) arrays for the design of efficient and low-cost Si inorganic solar cells. Despite their excellent light-absorbing characteristics,[1] the performance of SiNW-based all-inorganic solar cells are limited by severe surface recombination and low shunt resistance.[2] Encouragingly, Garnett et al. reported 5.3% power conversion efficiency (PCE) for a SiNW solar cell with a short-circuit current density (J_{sc}) higher than that of a similar cell based on planar Si.[1a] Recently, instead of using a fragile SiNW structure, Peng et al. demonstrated a mechanically more stable silicon nanohole solar cell with a high PCE of 9.51%.[3] The above two approaches require costly fabrication processes, such as deep reactive ion etching, thermal diffusion, or deep ultraviolet lithography. To address this concern, Si nanostructures have been incorporated with liquid electrolyte or organic semiconductors using much simpler and low-cost processes to fabricate photoelectrochemical cells[4] or solid-state hybrid heterojunction cells,[5] respectively. Recently, we have demonstrated a high-performance SiNW/poly(3,4-ethylene-dioxythiophene):polystyrenesulfonate (PEDOT:PSS) hybrid cell with a maximum PCE of 9%.[6] Although the PCE is higher than that of similar planar Si/PEDOT cell, which is mainly contributed by the much higher fill factor, the improvement in J_{sc} between the planar and SiNW cells is only marginal, from 24.5 to 26.3 mA/cm^2.

In this work, we report on Si/PEDOT hybrid cells based on synergistic surface texturing of SiNWs on pyramids. This geometry of SiNW/pyramid binary structure offers several advantages in the application of hybrid solar cells. Firstly, it increases the SiNW/PEDOT heterojunction area as compared to just an array of SiNWs on planar Si. Secondly, it is able to achieve excellent light trapping using only shorter SiNWs with a low aspect ratio, which suffer less aggregation than longer SiNWs and thus results in lower carrier recombination.[6,7] Moreover, shorter SiNWs have higher sturdiness as compared to longer SiNWs, thus leading to devices that are mechanically more robust. Using this SiNW/pyramid binary structure, our hybrid cells are found to have a maximum J_{sc} of 31.9 mA/cm^2 and PCE of 9.9%, which are much higher than that of similar cells based on planar Si, pyramid-textured Si, and SiNWs fabricated in this work for comparison. To the best of our knowledge, both the J_{sc} and PCE are the highest ever reported for hybrid cells based on Si nanostructures and PEDOT.

Figure 1a and b show the architectures of the binary structure of SiNWs on pyramid-textured Si and the completed

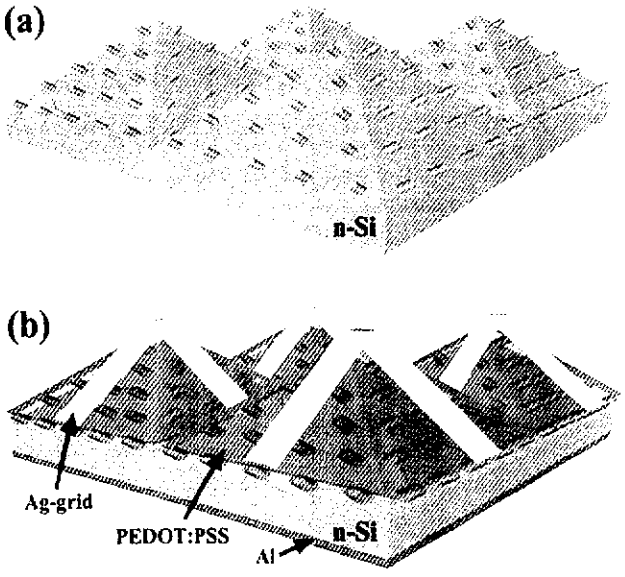

Figure 1. Architectures of a) SiNWs on the pyramid-textured Si binary structure, and b) the completed Si/PEDOT hybrid solar cell.

L. He, D. Lai, H. Wang, Prof. Rusli
School of Electrical and Electronic Engineering
Nanyang Technological University
50 Nanyang Avenue, 639798, Singapore,
CINTRA UMI CNRS/NTU/THALES 3288,
Research Techno Plaza, 637553, Singapore
E-mail: erusli@ntu.edu.sg

L. He, Dr. C. Jiang
Institute of Materials Research and Engineering
A*STAR, 3 Research Link, 117602, Singapore
E-mail: jiangc@imre.a-star.edu.sg

L. He, D. Lai, Prof. Rusli
CINTRA UMI CNRS/NTU/THALES 3288
Research Techno Plaza, 50 Nanyang Drive
Border X Block, Level 6, Singapore 637553

DOI: 10.1002/smll.201102095

Si/PEDOT hybrid cell structure, respectively. The binary structure was fabricated by a two-step chemical etching process. Firstly, randomly distributed upside pyramids were formed on 0.7–0.9 Ω cm N-type Si(100) wafer by anisotropic etching using potassium hydroxide and isopropanol solution. SiNW arrays with short lengths of 0.4 and 0.8 μm were then fabricated on the pyramid-textured substrate by electroless chemical etching in a solution of hydrofluoric acid and silver nitrate.[8] Highly conductive PEDOT:PSS was then spin-coated onto the binary structure to form the hybrid heterojunction. The rear and front electrodes were formed using evaporated aluminum layer on the backside of Si and silver grids on top of the PEDOT, respectively. Other hybrid cells based on planar Si, pyramid-textured Si, and SiNWs were also fabricated under identical condition for comparison.

Figure 2 shows the cross-sectional scanning electron microscopy (SEM) images of different textured Si structures. Figure 2a shows a planar Si coated with PEDOT which forms a uniform thin film of ~110 nm. Figure 2b shows the pyramid-textured Si with a base size of ~8 μm coated with PEDOT. It reveals that, due to gravitational force, the PEDOT solution tends to flow down to the bottom edges of the base of the pyramid. This results in a relatively thicker film of ~200 nm formed near the base edges and a much thinner layer <20 nm near the tips of the pyramids. Figure 2c and d show the SiNW arrays with different lengths of 0.4 and 0.8 μm, respectively, coated with PEDOT. The PEDOT forms a continuous thin film above the SiNW arrays, but its surface is rougher than that coated on the planar Si. Figure 2e and f show the as-prepared 0.4 μm SiNW arrays on pyramid-textured Si before and after being coated with PEDOT, respectively. Figure 2g and h show the corresponding images for the 0.8 μm SiNW sample. It is seen from Figure 2e and g that high-density and well-aligned SiNWs are formed perpendicular to all the sidewalls of the pyramids. Figure 2f and h demonstrate that the PEDOT is able to form a continuous canopy on the SiNWs even near the tip of the pyramid, owing to capillary action arising from the SiNW geometry. However, Figure 2h discloses that the 0.8 μm SiNW arrays result in a very non-uniform surface counter of the coated PEDOT, which is evidenced by the appearance of the protrusion of the SiNW tips.

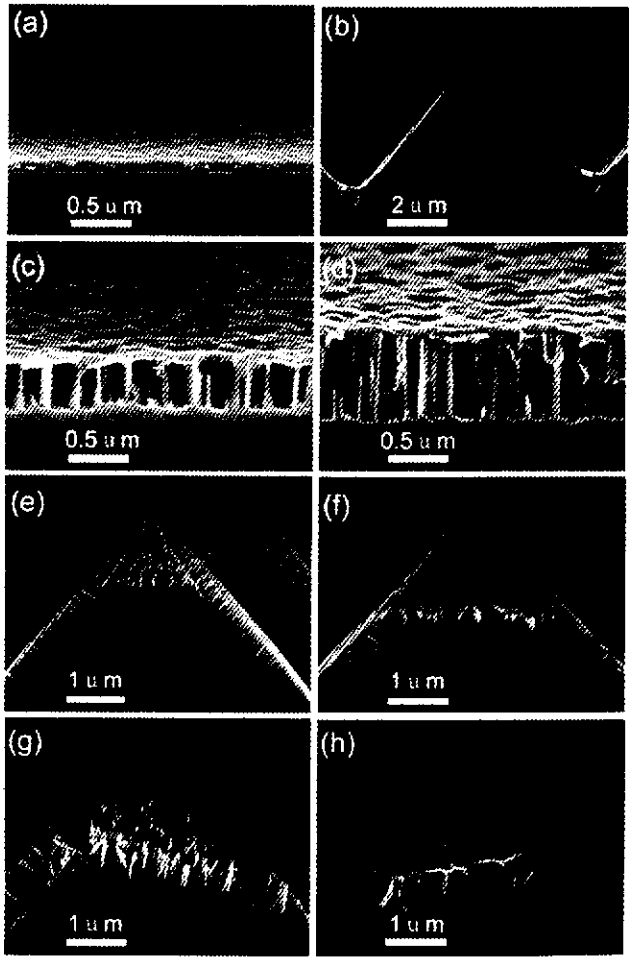

Figure 2. Cross-sectional view SEM images. The structure of a) planar Si, b) pyramid-textured Si, c) 0.4 μm SiNWs, and d) 0.8 μm SiNWs coated with PEDOT. e,f) 0.4 μm SiNWs on pyramid-texture Si before and after being coated with PEDOT. g,h) 0.8 μm SiNWs on pyramid-textured Si before and after being coated with PEDOT.

The reflectance spectra of different Si structures after being coated with PEDOT, measured using an integrating sphere by a Lambda 950 UV/Vis/NIR spectrophotometer system, are shown in **Figure 3**. It is seen that all the textured samples exhibit relatively lower reflectance than the planar Si sample. The pyramid-textured sample shows a reflectance of 6–18% over a wide spectrum from 350 to 1100 nm. As compared to planar Si and pyramid-textured Si, the reflectance of all the SiNW samples and binary structure samples is much lower, particularly over the range from 350 to 500 nm. This is because the nanoscale diameter of the SiNWs is of comparable dimension with these wavelengths of light, which thus boosts light scattering and prolongs the optical path length.[1a,c] The reflectance of the SiNW samples decreases as the SiNW length increases from 0.4 to 0.8 μm, which is expected due to the enhanced trapping of light by longer SiNWs. More importantly, the SiNW/pyramid binary structure significantly suppresses the reflectance to below 5% over a wide spectrum from 350 to 1100 nm. It exhibits the lowest reflectance among all the samples with different structures, attributed to the enhanced light trapping in a matrix

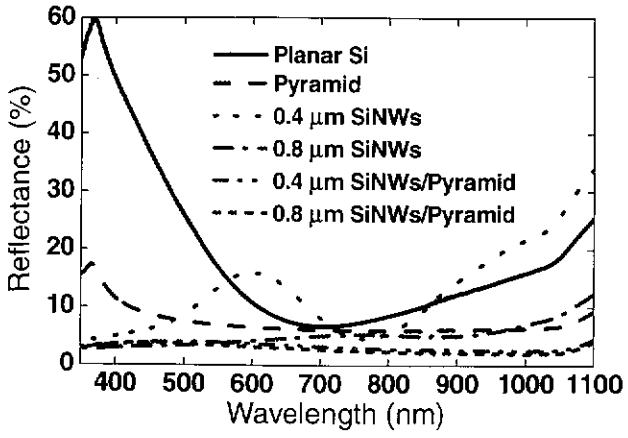

Figure 3. Reflectance of planar Si, pyramid-textured Si, SiNWs, and pyramid/SiNW binary structure coated with PEDOT.

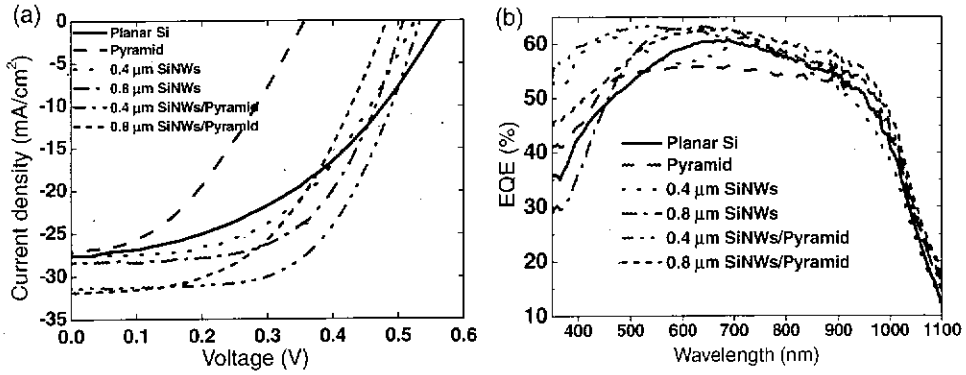

Figure 4. a) The *J–V* characteristics of the hybrid cells with different Si structures fabricated under the same conditions. b) The EQE of the hybrid cells with different Si structures.

of antireflection components combining both pyramids and SiNWs.

Figure 4a shows the (current density)–voltage (*J–V*) characteristics of the hybrid cells with different Si structures under simulated AM 1.5G irradiation at 100 mW/cm^2 derived from a solar simulator. The Si/PEDOT hybrid cell could be modeled as a Schottky-type device formed by inorganic semiconductor/conductive polymer heterojunction[9] since PEDOT is highly conductive. Si is the primary light absorber and the medium for photo-excited electrons transport, whereas PEDOT is an electrode for the transport of holes. The photovoltaic parameters of short circuit (J_{sc}), open-circuit voltage (V_{oc}), fill factor (FF), and PCE are presented in **Table 1**. It is seen that a good PCE of 7.0% has been obtained by the planar Si/PEDOT cell, which demonstrates an excellent heterojunction formed between Si and PEDOT. The 0.4 μm SiNW/pyramid binary structure exhibits the highest PCE of 9.9% among all the structures. It is worth noting that the light absorption in the underlying Si substrate will contribute to the photocurrent of the cells, whereas the SiNW/pyramid binary structure will enhance the trapping of light and the photocurrent generated. The pyramid-textured cell on the other hand shows the worst PCE of 3.9% due to its much lower V_{oc} and FF. The PEDOT layer near the tips of the pyramids in this structure is very thin (Figure 2b) such that there may be direct contact between the Si pyramids and the top silver electrode. This will lead to a low shunt resistance and thus reduced V_{oc} and FF. As compared to the planar Si cell, the PCE of the cells with 0.4 and 0.8 μm SiNWs increase from 7.0% to 7.8% and 8.5%, respectively, attributed to an improvement in their FF. This could be ascribed to the shorter diffusion distance of photo-excited minority carriers from the junction formed on the SiNW arrays.[10] It is also noted that despite their lower reflectance (Figure 3), the SiNW cells exhibit similar J_{sc} as the planar Si cell. This is consistent with what we have reported previously and it is attributed to the higher carrier recombination loss associated with the uncovered sidewalls of the SiNWs.[6] On the other hand, both the 0.4 and 0.8 μm SiNW/pyramid binary structure cells exhibit remarkably improved J_{sc} of 31.4 and 31.9 mA/cm^2, respectively. As compared to the structures based on SiNWs, the binary structures with similar SiNW lengths have a considerable 12% enhancement in the J_{sc}, attributed to their much lower reflectance (Figure 3). Figure 4b exhibits the external quantum efficiency (EQE) of the hybrid cells fabricated with different Si structures. It is shown that in line with their much higher J_{sc}, the 0.4 and 0.8 μm SiNW/pyramid binary structures in general exhibit a stronger spectral response than the other structures over the wide spectrum from 350 to 1100 nm. However, the PCE of the binary structure cell with 0.8 μm SiNWs is only 7.7%, which is less than 9.9% for the binary structure cell with 0.4 μm SiNWs, as a result of its lower V_{oc} and FF. This could be ascribed to local shunting across the cells at the regions where there is protrusion of the longer SiNW tips (Figure 2h) close to the top electrode. The drop in V_{oc} for cells with longer SiNWs is also attributed to higher carriers recombination associated with their increased surface area. The defective surface of the SiNWs prepared by electroless etching[11] and the poor infiltration and coverage of PEDOT[6] onto the SiNW surface will exacerbate carrier recombination and lower the V_{oc}.

Table 2 summarizes the up-to-date reported hybrid solar cells based on Si nanostructures and different organic materials. It is seen that only the surface texturing using SiNW arrays has been reported so far. Our hybrid cell based on the SiNW/pyramid binary structure demonstrates the second highest PCE of 9.9% and the highest J_{sc} of 31.9 mA/cm^2 to date. Besides the excellent light capturing capability, the reduced surface defects and carrier recombination associated with the low-aspect-ratio SiNWs are the key advantages of the SiNW/pyramid geometry.

Table 1. Summary of photovoltaic parameters of the hybrid cells with different structures.

Sample	J_{sc} [mA/cm^2]	V_{oc} [V]	FF [%]	PCE [%]
Planar Si	27.6	0.55	46.3	7.0
Pyramid	27.1	0.36	39.8	3.9
0.4 μm SiNWs	27.7	0.52	54.4	7.8
0.8 μm SiNWs	28.4	0.51	58.9	8.5
0.4 um SiNWs/ pyramid	31.4	0.53	59.3	9.9
0.8 μm SiNWs/ pyramid	31.9	0.48	50.3	7.7

small

Table 2. Summary of up-to-date reported hybrid solar cells based on Si nanostructures and organic materials.

Si structure	Organic material	Group/year	PCE [%]	J_{sc} [mA/cm^2]
SiNW	Poly(3-octylthiophene) (P3OT)	G. Kalita et al./2010[5a]	0.61	7.85
SiNW	PEDOT:PSS	S.-C. Shiu et al./2010[5b]	5.08	19.28
SiNW	Poly(3-hexylthiophene) (P3HT)	F. Zhang et al./2011[5c]	5.9	26.2
SiNW	Spiro-OMeTAD/PEDOT:PSS	L. He et al./2011[5d]	10.3	30.9
SiNW	PEDOT:PSS	L. He et al./2011[6]	9.0	26.3
SiNW	PEDOT:PSS	B. Ozdemir et al./2011[5e]	5.3	30.2
SiNW/Pyramid	PEDOT:PSS	L. He et al./2012 (this work)	9.9	31.9

In conclusion, we have demonstrated a simple approach to fabricate an efficient Si/PEDOT hybrid cell using a synergistic surface texturing of SiNWs on pyramids forming a binary structure. Hybrid cells based on other structures such as planar Si, pyramid-textured Si, and SiNWs are also fabricated for comparison. The binary structure exhibits the lowest reflectance of less than 5% over a wide spectrum from 350 to 1100 nm. Despite a 12% shadowing loss and the absence of back surface field enhancement, the hybrid cell based on the binary structure demonstrates the highest J_{sc} of 31.9 mA/cm^2 and PCE of 9.9%, much higher than those of the other structures investigated. The PCE will be up to 11.2% if the silver grid covered area is not considered. The expensive Si substrates have been used in this work to conveniently demonstrate the Si/polymer hybrid concept, rather than as the final platform where such devices will be built. For practical applications, we envisage that ultimately such Si/PEDOT hybrid cells will have to be built using Si or poly-Si thin films deposited on low-cost substrates to bypass the use of costly bulk Si wafers. Indeed the fabrication process used in this work can be easily adapted to Si thin films. Despite the potential instability of such hybrid devices owing to the use of organic material, there is still strong motivation for research into such hybrid cells because of the low cost, low temperature, and process simplicity that they offer. Furthermore the stability issue could be alleviated by having good encapsulation. Overall, owing to the excellent light trapping induced by synergistic micro-/nanoscale surface texturing and the simple processing of the organic materials, such a pyramid/SiNW/PEDOT composition has potential to realize low-cost and efficient Si/organic hybrid solar cells.

Experimental Section

Fabrication of Pyramid-Textured Si: The starting wafer used to fabricate the solar cells was single-crystal, N-type Si(100) with resistivity of 0.7–0.9 Ω cm. The wafers were sequentially cleaned in acetone, ethanol and deionized (DI) water for 10 min each at room temperature. The randomly distributed upside pyramid structures were fabricated by anisotropic etching of Si in a mixture solution of potassium hydroxide (KOH) (5 wt.%) and isopropanol (5 vol.%) at 85 °C for 30 min. The textured Si substrates were then immersed in dilute hydrochloric acid for 1 h and hydrofluoric acid (HF) for 10 min to remove any residue KOH and silicon dioxide, respectively.

Fabrication of SiNW Arrays on Pyramid-Textured Si: The pyramid-textured Si substrates were sequentially cleaned in acetone, ethanol and DI water for 10 min each at room temperature. The cleaned substrates were then immersed in an etching solution of 4.6 M HF and 0.02 M $AgNO_3$ at room temperature to form SiNWs. The as-prepared SiNWs were soaked in concentrated nitric acid for at least 30 min to dissolve the silver dendrites. Finally, all the samples were immersed in dilute aqueous HF acid to remove the oxide.

Fabrication of Si/PEDOT Hybrid Solar Cells: After the fabrication of SiNW arrays on pyramid-textured Si substrates, the rear electrode was formed by electron-beam evaporation of 300 nm thick aluminum onto the backside of the Si substrates. Highly conductive PEDOT:PSS (Clevios PH500) mixed with dimethyl sulfoxide (5 wt.%) was spin-coated on the samples and then annealed at 110 °C for 10 min at atmosphere. Silver metal grids were deposited on top of the PEDOT layer by electron-beam evaporation through a shadow mask. The fraction of the silver grids shading area is 12%. Each sample has a device area of 0.95 cm^2. Other hybrid cells based on planar Si, pyramid-textured Si, and SiNWs were fabricated under identical condition for comparison.

Characterization of the Samples: The cross-sectional topography of different Si structures was measured using field-emission SEM (FESEM). The reflectance spectra of the different Si structures coated with PEDOT layer were characterized using an integrating sphere by a PerkinElmer Lambda 950 UV/Vis/NIR spectrophotometer system. The photovoltaic *J–V* characteristics of the cells were measured with a Keithley 2400 Source-Meter unit under 100 mW/cm^2 illumination (AM 1.5G) from a solar simulator (San-El electric). The intensity of the light source was calibrated by a Si reference cell which is traceable both to the National Renewable Energy Laboratory (NREL), and to the International System of Units (SI). The EQE was measured with a characterization system consisting of a Xenon lamp, a chopper controller, a monochromator, and a lock-in amplifier.

Acknowledgements

*This work was supported by A*STAR, Singapore under Grant No: 092 101 0055.*

[1] a) E. Garnett, P. Yang, *Nano Lett.* **2010**, *10*, 1082; b) M. D. Kelzenberg, S. W. Boettcher, J. A. Petykiewicz, D. B. Turner-Evans, M. C. Putnam, E. L. Warren, J. M. Spurgeon, R. M. Briggs, N. S. Lewis, H. A. Atwater, *Nat. Mater.* **2010**, *9*, 239; c) H. Lu, C. Gang, *Nano Lett.* **2007**, *7*, 3249; d) J. Zhu, Z. Yu, G. F. Burkhart, C.-M. Hsu, S. T. Connor, Y. Xu, Q. Wang, M. McGehee, S. Fan, Y. Cui, *Nano Lett.* **2009**, *9*, 279; e) L. Junshuai, Y. HongYu, W. She Mein, Z. Gang, S. Xiaowei, P. G. Q. Lo, K. Dim-Lee, *Appl. Phys. Lett.* **2009**, *95*, 033102.

[2] a) L. Tsakalakos, J. Balch, J. Fronheiser, B. A. Korevaar, O. Sulima, J. Rand, *Appl. Phys. Lett.* **2007**, *91*, 233117; b) E. C. Garnett, P. Yang, *J. Am. Chem. Soc.* **2008**, *130*, 9224; c) C. E. Kendrick, H. P. Yoon, Y. A. Yuwen, G. D. Barber, S. Haoting, T. E. Mallouk, E. C. Dickey, T. S. Mayer, J. M. Redwing, *Appl. Phys. Lett.* *97*, 143108; d) V. Sivakov, G. Andra, A. Gawlik, A. Berger, J. Plentz, F. Falk, S. H. Christiansen, *Nano Lett.* **2009**, *9*, 1549; e) O. Gunawan, S. Guha, *Sol. Energy Mater. Sol. Cells* **2009**, *93*, 1388.

[3] K.-Q. Peng, X. Wang, L. Li, X.-L. Wu, S.-T. Lee, *J. Am. Chem. Soc.* **2010**, *132*, 6872.

[4] a) A. P. Goodey, S. M. Eichfeld, K.-K. Lew, J. M. Redwing, T. E. Mallouk, *J. Am. Chem. Soc.* **2007**, *129*, 12344; b) K.-Q. Peng, X. Wang, X.-L. Wu, S.-T. Lee, *Nano Lett.* **2009**, *9*, 3704; c) X. Shen, B. Sun, F. Yan, J. Zhao, F. Zhang, S. Wang, X. Zhu, S. Lee, *ACS Nano* **2010**, *4*, 5869; d) X. Wang, K.-Q. Peng, X.-J. Pan, X. Chen, Y. Yang, L. Li, X.-M. Meng, W.-J. Zhang, S.-T. Lee, *Angew. Chem. Int. Ed.* **2011**, *50*, 9861; e) P. Kuiqing, W. Xin, L. Shuit-Tong, *Appl. Phys. Lett.* **2008**, *92*, 163103.

[5] a) G. Kalita, S. Adhikari, H. R. Aryal, R. Afre, T. Soga, M. Sharon, W. Koichi, M. Umeno, *J. Phys. D: Appl. Phys.* **2009**, *42*, 115104; b) S.-C. Shiu, J.-J. Chao, S.-C. Hung, C.-L. Yeh, C.-F. Lin, *Chem. Mater.* **2010**, *22*, 3108; c) F. Zhang, B. Sun, T. Song, X. Zhu, S. Lee, *Chem. Mater.* **2011**, *23*, 2084; d) L. He, C. Jiang, Rusli, D. Lai, H. Wang, *Appl. Phys. Lett.* **2011**, *99*, 021104; e) B. Ozdemir, M. Kulakci, R. Turan, H. E. Unalan, *Appl. Phys. Lett.* **2011**, *99*, 113510; f) A. A. D. T. Adikaari, D. M. N. M. Dissanayake, R. A. Hatton, S. R. P. Silva, *Appl. Phys. Lett.* **2007**, *90*, 203514.

[6] L. He, Rusli, C. Jiang, H. Wang, D. Lai, *IEEE Electron Device Lett.* **2011**, *32*, 1406.

[7] H. Li, R. Jia, C. Chen, Z. Xing, W. Ding, Y. Meng, D. Wu, X. Liu, T. Ye, *Appl. Phys. Lett. 98*, 151116.

[8] K.-Q. Peng, Y. Xu, Y. Wu, Y. Yan, S.-T. Lee, J. Zhu, *Small* **2005**, *1*, 1062.

[9] a) M. J. Sailor, F. L. Klavetter, R. H. Grubbs, N. S. Lewis, *Nature* **1990**, *346*, 155; b) D. P. Halliday, J. W. Gray, P. N. Adams, A. P. Monkman, *Synth. Metals* **1999**, *102*, 877.

[10] K.-Q. Peng, S.-T. Lee, *Adv. Mater.* **2011**, *23*, 198.

[11] A. I. Hochbaum, R. Chen, R. D. Delgado, L. Wenjie, E. C. Garnett, M. Najarian, A. Majumdar, Y. Peidong, *Nature* **2008**, *451*, 163.

Received: October 5, 2011
Revised: January 20, 2012
Published online: March 21, 2012

